

## The effect of layered silicates on the morphological, rheological and mechanical properties of PA and PP blends

Qodirbek Nuridin ugli Berdinazarov<sup>1,a</sup>, Elshod Olmosovich Khakberdiev<sup>1,b</sup>,  
Nigmat Rustamovich Ashurov<sup>1,c</sup>

<sup>1</sup>Institute of Polymer Chemistry and Physics, Uzbekistan Academy of Sciences, Tashkent, Uzbekistan

<sup>a</sup>qodirberdinazarov@mail.ru, <sup>b</sup>profhaqberdiyev@gmail.com, <sup>c</sup>nigmat.ashurov@gmail.com

Corresponding author: Q. Berdinazarov, qodirberdinazarov@mail.ru

PACS 83.80.Tc, 82.35.Np, 82.35.Lr

**ABSTRACT** We study rheological, morphological and mechanical properties of polyamide-6 (PA) and polypropylene (PP) blends in the presence of layered silicates (two types of organically modified montmorillonite - Cloisite30B for PA and Cloisite20A for PP). For comparison, we used maleic anhydride grafted polypropylene (PP-g-MA) as a compatibilizer and in all compositions weight ratio of PA and PP was constant 80/20, respectively. Introduction of layered silicates always led to more viscous melt and increased storage modulus. It is also identified that layered silicates cause more finer-dispersed morphology than PP-g-MA. Elastic modulus and yield strength were increased when the layered silicates were introduced in either composites or blends.

**KEYWORDS** Polyamide-6, polypropylene, montmorillonite, polymer composite, polymer blend, compatibilizer

**ACKNOWLEDGEMENTS** The authors acknowledge prof. Paula Moldenaers and her SMaRT team for their assistance in conducting practical experiments. The study was financed by the project of "Nanocomposite polymer-polymer blend materials on the basis of polyolefins produced in Uzbekistan".

**FOR CITATION** Berdinazarov Q., Khakberdiev E., Ashurov N. The effect of layered silicates on the morphological, rheological and mechanical properties of PA and PP blends. *Nanosystems: Phys. Chem. Math.*, 2024, **15** (3), 410–417.

### 1. Introduction

Blends of polyamide (PA) and polypropylene (PP) have gained significant prominence in various industrial applications due to their multifaceted advantages. Combining the inherent chemical resistance of PA with the lightweight characteristics of PP results in a material that not only exhibits robust resistance to a variety of chemicals but also facilitates weight reduction in applications where mass is a crucial factor. Furthermore, the synergistic combination of these polymers contributes to enhanced thermal stability, making the blend suitable for applications demanding resilience to elevated temperatures. The incorporation of cost-effective PP into the blend not only reduces overall material costs but also imparts improved mechanical properties by balancing the high tensile strength and impact resistance of PA with the stiffness of PP. This combination of chemical resistance, weight reduction, enhanced thermal stability, cost reduction, and improved mechanical properties positions PA-PP blends as versatile and economically viable solutions across diverse industrial sectors. Aside from their common applications in automobile interior and exterior components such as dashboard panels, door trims, bumpers, and wheel arch liners, PP/PA blends prove invaluable under the hood as well. With their notable heat resistance and durability, these blends find ideal use in critical under-the-hood components like air intake manifolds [1, 2]. Furthermore, their exceptional thermal stability and resistance to automotive fluids render them suitable candidates for engine covers, contributing to the reliable performance and longevity of automotive engines [3, 4].

At the same time, the incompatibility of these polymer pairs limits the achievement of the set goals. The incompatibility of polymers is rooted in low interfacial adhesion; conversely, high interfacial tension exacerbates this issue [5–8]. The solution to this problem has been demonstrated in numerous compatibilization experiments, wherein a third functionalized polymer is introduced to enhance compatibility with one of the components of the blend and react effectively with the other component. This approach is called reactive compatibilization, forming a copolymer (graft or block copolymer), as a rule, reaches the phase boundary and prevents the process of coalescence of particles of the dispersed phase and stabilizes the desired blend morphology [9, 10]. The implementation of such an approach to the PA and PP pairs by using compatibilizers such as maleic anhydride grafted PP (PP-g-MA) or ethylene-polypropylene copolymer can significantly reduce the water absorption of PA and significantly increase the dimensional stability and impact resistance of the polymer blend [11–13].

Another important approach is the introduction of nanosized non-organic fillers into polymer blends, among which layered silicates occupy a special place. Dispersion of particles of layered silicate to nanosizes (particles in the form of

discs with a thickness of less than one nanometer and a perimeter is approximately 100 nm) or intercalation of macromolecules into the interlayer space of layered silicate allows a very significant increase in the elastic modulus, yield strength, and reduces permeability [14, 15].

Composites in which the necessary levels of specific interaction with the surface of the particles of layered silicate and modifier are provided lead to the formation of exfoliated and intercalated nanocomposites, respectively. Specific interaction is easily achieved for polar PA, while polyolefins require the introduction of a certain proportion of a functionalized polymer, that is, a compatibilizer, for which the earlier maleic anhydride grafted polyolefins have proven to be effective [16].

The combination of these two approaches for a PA/PP blend has been the subject of a number of studies [17–20]. At the same time, in many works, the components of the blend, two polymers and particles of layered silicate, and in some cases with the addition of functionalized PP for compounding, were loaded into the extruder at the same time. This method was initiated in work [21], in which it was shown that the introduction of nanosized inorganic third particles in a blend of polymers leads to their indication at the phase boundary, that is, a compatibilizing effect was discovered. Depending on the degree of polarity, the mixing of blend components and the type of modifier of the organically modified layered silicate, the particles can be located in one of the phases, in two phases simultaneously or at the phase boundary [22].

The compatibilizing effect, which is manifested in the case of particles of layered silicate in one of the polymer phases, especially dispersed, the other two cases determine the possibility of transition from dispersed morphology to coexisting two continuous phases and changing the pattern over the phases. A slightly different, combined method for the formation of PA/PP polymer blends in the presence of modified montmorillonite (MMT) has been proposed [21]. The difference is that the first family of compositions was obtained in one stage (introduction of the blend components, simultaneous), in second the approach - the compositions were obtained in two stages, that is the second polymer (PA or PP) was extruded with finished compositions in the second stage. That is, the authors, as it were, considered 2 variants of components based on PA/PP with the introduction of a modified MMT in the presence and absence of a compatibilizer (PP-g-MA). In all cases, with the exception of the two-stage variant of obtaining the composition of PA and organically modified (OMMMT) at the first stage and with the subsequent addition of PP, the authors observed the formation of various levels of intercalated structures. Moreover, the same composition, with the addition of a compatibilizer, formed only an intercalated structure. The mechanism of such a phenomenon was not disclosed in the work. Unfortunately, the authors of the work did not present the characteristics of the layered silicate sample, one thing is clear that these particles are concentrated in the PA phase. The authors formulate the final conclusions as follows: finer dispersion of layered silicate particles leads to a noticeable increase in the elastic modulus up to 42%, while compatibilization of a blend of two polymers contributes to an increase in the yield strength of nanocomposite polymer blends. In addition to this, the authors did not take into account the formation of a third polymer phase in the form of a well-known copolymer of PA with PP-g-MA. As noted by the authors of the work [23, 24], this copolymer not only contributes to the increase in interfacial adhesion between PA and PP, but also to a certain extent they are preferential territories for the introduction of layered silicate particles.

In this work, the PA:PP blend in 80:20 ratio was selected as the most favorable after evaluating the physicochemical characteristics across a range of sample compositions we also chose a two-stage variant preparation of the PA/PP polymer blends. At the first stage, a sample was obtained from pure components, separately compositions of PA/PP with OMMMT (Cloisite20A and Cloisite30B, respectively, in the presence and absence of a compatibilizer in the form of PP-g-MA), at the second stage, various compatibilization of PA and PP were mixed in the ratio of 80/20 wt.%. Knowledge of the initial structures and their transformation into mixing processes made it possible to establish the correlation dependences between the rheological characteristics, the features of the structure and morphology of the blends, and the final elastic-strength properties of multi-component nanostructured systems based on PA and PP.

## 2. Experimental

PA6, Toplon grade 1027 BRT, with  $M_w = 80$  kDa, relative viscosity 2.7 was purchased. Isotactic PP (J-170T) with  $M_w = 200$  kDa, MFI = (2.16 kg, 230°C) 21 g/10 min was kindly provided by JV Uz-Kor Gas Chemical LLC. PP-g-MA with 2.5 wt.% maleic anhydride content and MFI = (2.16 kg, 230°C) >200 g/min was provided by JV UzAuto CE-PLA LLC, as a gift. Cloisite30B, (spacing  $d_{001} = 1.83$  nm, methylbis(2-hydroxyethyl)-tallow ammonium chloride conc. 0.9 mEq/g) and Cloisite20A, (spacing  $d_{001} = 247$  nm., dimethyl dehydrogenated tallow ammonium conc. 0.95 mEq/g) Southern Clay Products, Inc., Gonzales, TX were used. The particle size in both clay types is less than 13  $\mu\text{m}$ . Cloisite 20A and Cloisite 30B are modified montmorillonite clays through the incorporation of quaternary ammonium salts. Cloisite 20A is enriched with dimethyl dihydrogenated tallow ammonium chloride, while Cloisite 30B contains methyl tallow bis-2-hydroxyethyl ammonium chloride. Tallow, sourced from beef, primarily consists of carbon chains with 18 carbons (about 65% C18, approximately 30% C16, and roughly 5% C14). Hydrogenated tallow is obtained from tallow through the hydrogenation process, eliminating double bonds. With two tallow groups, Cloisite 20A exhibits greater hydrophobicity compared to Cloisite 30B.

Prior to obtaining the composites and blends by melt-blending, PA was dried under vacuum overnight at 80°C. The melt-blending process was performed using a conical co-rotating fully intermeshing twin-screw midi-extruder (DSM

Research, The Netherlands). On the first stage, PA and PP nanocomposites and their blends in the absence and presence of PP-g-MA were obtained, listed in Table 1. On the second stage, PAClay and PPCLay, were mixed separately with pure PA and PP, as well as together without pure components (Table 2). The compositions of PAClay and PPCLay composites shown in Table 2 were subjected to the same processing as the second cycle. The melt-blending process was carried out for 5 minutes at 50 rpm and at temperature profiles of 230, 235, and 240 °C. The dog bone shaped specimens for mechanical experiments are obtained on Laboratory injection molding machine of ZAMAK Mercator 1947 (Poland) and the and dimensions of the specimen were illustrated in details elsewhere [25].

TABLE 1. Composition of polymer composites and blends

	PA	PP	PP-g-MA	Cloisite20A	Cloisite30B
PPCLay	–	91	6	3	–
PAClay	97	–	–	–	3
PA/PP 80/20	80	20	–	–	–
PA/PP/PP-g-MA 72/18/10	72	18	10	–	–

TABLE 2. Composition of polymer blends (subjected the second cycle)

	PAClay	PPCLay	PA	PP
PA/PPCLay 80/20	–	20	80	–
PAClay/PP 80/20	80	–	–	20
PAClay/PPCLay 80/20	80	20	80	–

XRD measurements were conducted with Rigaku Miniflex 600, the condition of 40 kV voltage, 15 mA current and 0.02° step. The measurements were carried out from 2° to 30°, and interplanar distances were calculated according to Bragg's law using SmartLab Studio II.

$$n\lambda = 2d \sin \theta$$

where,  $n$  is the diffraction order,  $\lambda$  is the wavelength of X-ray (1.5406 Å),  $\theta$  is the incident angle, and  $d$  is the interplanar distance.

Rheological tests were carried out on TA instruments ARES-2K strain controlled remoter in nitrogen atmosphere, at 240 °C. Frequency sweep and time sweep were done in linear regime. Tensile tests were conducted according to ASTM D 638 in Shimadzu AG-X PLUS (Japan). For measuring tensile module ( $E$ ), 1 mm/min crosshead speed was chosen until 0.3 % deformation, after that crosshead speed increased immediately to 20 mm/min for further exploration yield stress ( $\sigma$ ) and deformation ( $\varepsilon$ ). The morphological properties of obtained samples were investigated on JEOL JSM-6010LM SEM, at 20 kV accelerating voltage. Before visualization, all samples were coated with a thin Au/Pd layer by JEOL JFC-1300 autofine coater (JEOL, Lireweg, The Netherlands) on order to avoid charging during imaging.

### 3. Results and discussions

#### 3.1. X-ray diffraction (XRD) measurements

XRD patterns of PA, Cloisite30B and their composites are illustrated in Fig. 1. Interlayer distance accounts for 18.29 Å in Cloisite30B which corresponds to intensive peak in 4.83°. In the XRD pattern of PAClay composite, this peak becomes a flat, indicating exfoliated structure.

With regard to PP and its composite with Cloisite20A, XRD results show intercalation of clay particles within PP matrix (Fig. 2). Interlayer distance  $d$  increases from 24.66 to 34.75 Å as a result of insertion of PP macromolecules into between clay platelets. Even though in our previous work, we obtained exfoliated structure for the same composition due to the difference between processing conditions, intercalated nanostructures were identified by XRD measurements. Moreover, distribution of clay particles in polymer matrix affected crystallization behavior of the polymer. In both cases, nucleating effect led to increase intensity of the crystallization peak. In PA, alone peak in 21,5° and in PP, peak i 16.9° increased remarkably, contributing more perfect crystallization.

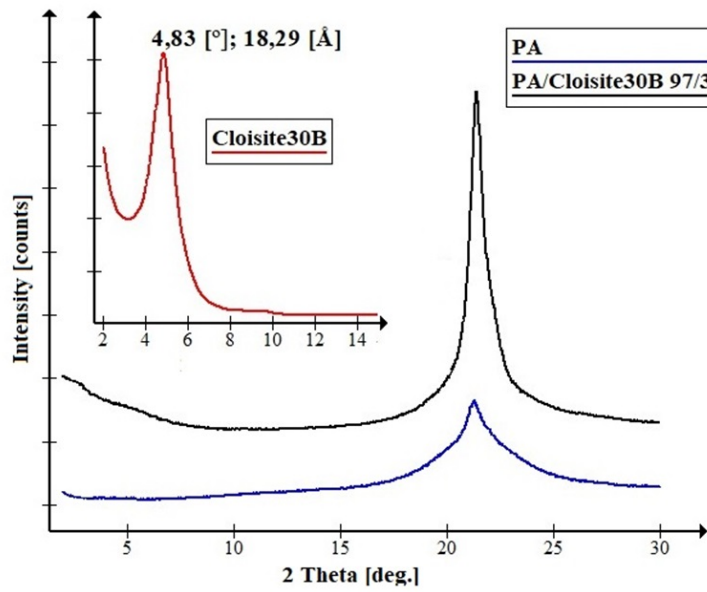


FIG. 1. XRD patterns of PA, Cloisite30B and their composites

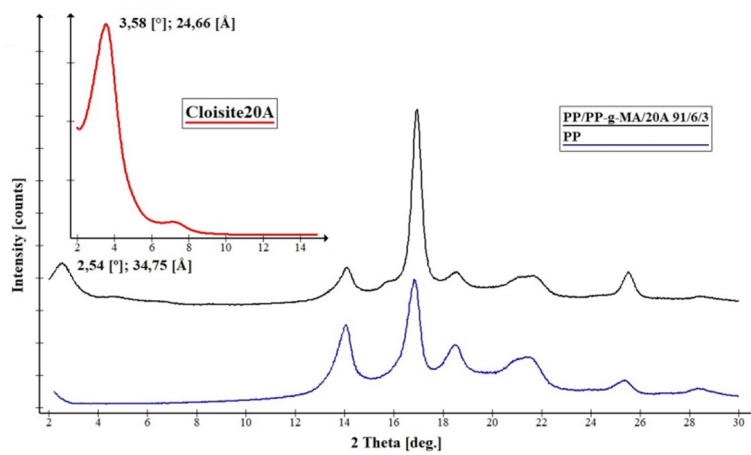


FIG. 2. XRD patterns of PP, Cloisite20A and their composites

### 3.2. Rheological measurements

In Fig. 3, the dependencies of complex viscosity and dynamic modulus of the initial components in blends and nanocomposites based on PA and PP with modified MMT are presented as an example against shear rate (frequency sweep). Similar curves were obtained for all investigated compositions, and viscosity values for three velocity gradients.

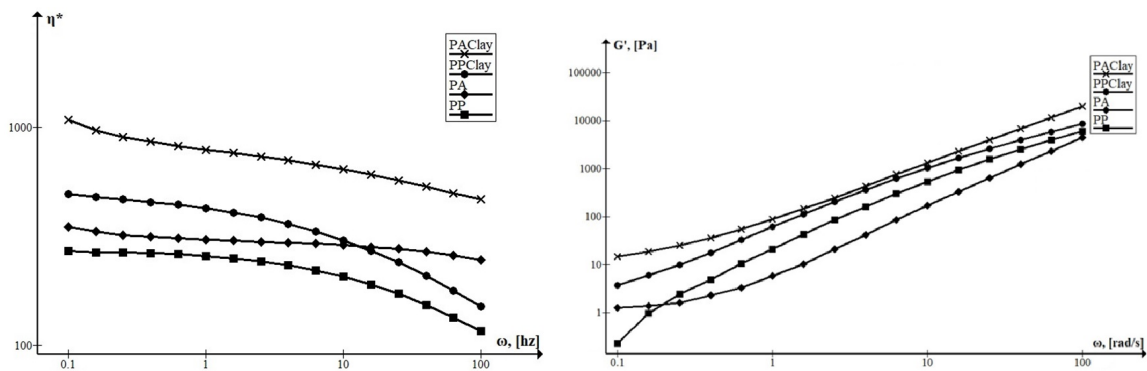


FIG. 3. Complex viscosity and storage modulus of PA, PP and their nanocomposites with 3 wt. % of clay

It is also known [19, 26] that the viscosity of melt nanocomposites is highly sensitive to the degree of dispersion of layered silicate particles, i.e., the aspect ratio, which in turn directly depends on the level of macromolecule intercalation into the interlayer space of the MMT, up to the exfoliation of the latter into individual nanoscale plates, the anisotropy coefficient of which is maximal. The viscosity values of exfoliated PA nanocomposites are significantly higher throughout the range of shear rate gradients compared to intercalated PP nanocomposites.

In Fig. 4., complex viscosity and storage modulus of 5 blends are shown. As expected, for all blend compositions, the complex viscosity decreases with an increase in shear rate [27, 28]. Upon the introduction of a compatibilizer and nanocomposites based on the virgin components, the complex viscosity notably increases. The highest viscosities to blends in which the original components are replaced with corresponding nanocomposites and, in place of the PP phase, an intercalated PP nanocomposite, respectively. As is hypothesized, such rheological behavior is associated with the structuring of the composition during the mixing process, that is, with the emergence of varying levels of specific interactions between components. In PA/PPClay blend, an intercalated PP nanocomposite is present, which was obtained by introducing 6 wt.% PP-g-MA. It is known that PP-g-MA reacts with PA macromolecules, forming a grafted copolymer of PA with PP [29]. Apparently, the structuring and degradation of PP under the selected temperature conditions of mixing also contribute to this process [30].

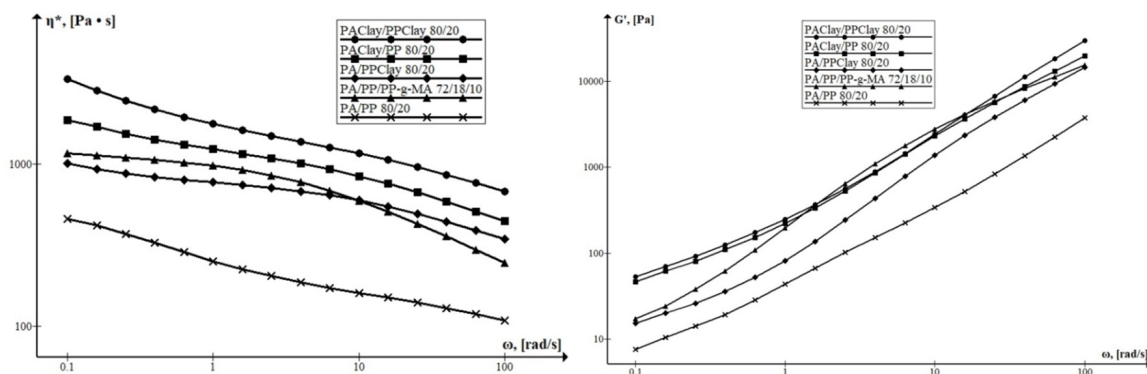


FIG. 4. Complex viscosity and storage modulus of PA/PP blends

### 3.3. Morphological investigations

Analysis of the cryo-fractured surface of the samples under SEM revealed that the particle size of the dispersed phase compared to samples of PA/PP blends indicates that the compatibilized blend is 7–8 times smaller than that of a conventional one (Fig. 5). Thanks to good interfacial adhesion resulting from the presence of a reaction between the amino group of PA and PP-g-MA, leading to the formation of a grafted copolymer, the particles of the PP dispersed phase remain bound to the PA matrix during the low-temperature fracture process. For blends of samples without a compatibilizer, particles of the dispersed phase torn from the surface are clearly seen. For a PA/PPClay, the size of the particles of the dispersed phase uniformly distributed in the PA phase is  $500 \pm 150$  nm on average (Fig. 3c,d).

The intercalated PP nanocomposite acts as a more effective compatibilizer in comparison with the classical PP-g-MA for this blend of polymers.

The replacement of the PA phase with exfoliated PA nanocomposite also brings an insignificant compatibilizing effect (Fig. 5e,f). The sizes of the dispersed PP phase exhibit a broad particle size distribution ranging from 1 – 8  $\mu\text{m}$ , contrasting with conventional blends where these sizes vary within the range of 3 – 14  $\mu\text{m}$ . The absence of a pronounced effect of compatibilization is apparently due to the fact that exfoliated MMT particles are distributed in the bulk of the PA phase and practically does not participate in the processes of coalescence of the dispersed phase particles.

### 3.4. Mechanical analysis

It is well known that blending two incompatible polymers can result in different expressions of final mechanical properties, depending on the blend composition, individual polymer characteristics, and blend morphology [31]. In the case of nanocomposites based on layered silicates, besides interfacial adhesion, the elastic-strength characteristics, particularly the modulus of elasticity, are influenced by the dispersion of modified MMT, meaning the anisotropy coefficient (aspect ratio – the ratio of particle length to thickness).

The mechanical properties such as the elastic modulus (E), the yield strength ( $\sigma$ ), and the relative elongation at break ( $\epsilon$ ) of PA and PP, along with the nanocomposites containing Cloisite30B and Cloisite20A, as well as their blends are outlined in Table 3. We will analyze how these parameters change as we transit from individual components to multi-component compositions.

The initial modulus of elasticity slightly differs (higher for PA), with an increase of 10 % for the intercalated PP nanocomposite and over 50% enhancement in the modulus of elasticity for the exfoliated PA nanocomposite, consistent

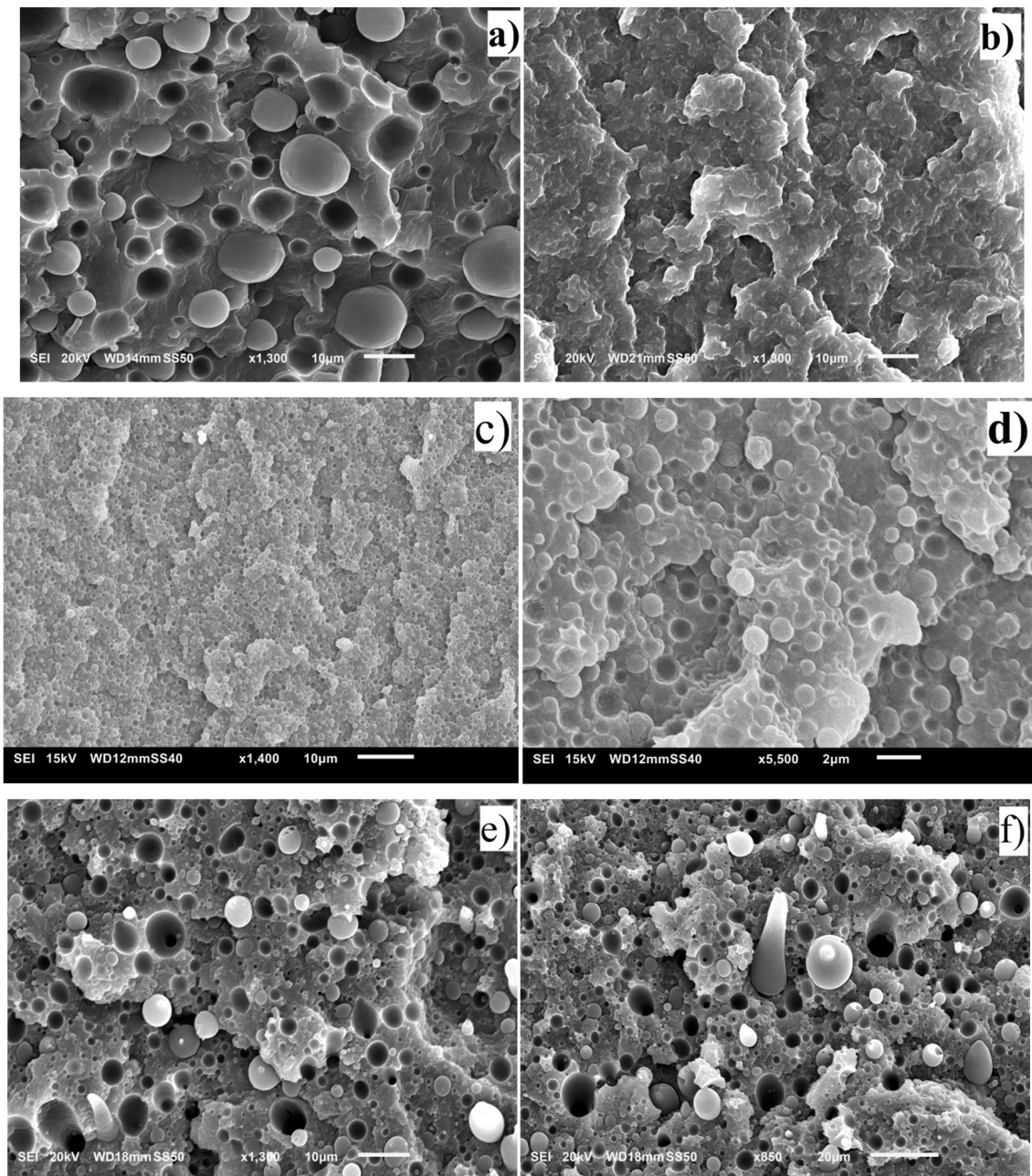


FIG. 5. SEM images of PA/PP blends 80/20 ratio series. a) PA/PP, b) PA/PP/PP-g-MA, c) and d) PA/PP/clay, e) and f) PA/clay/PP

with similar findings reported in previous studies [32]. A minor enhancement effect in terms of yield strength is observed in the corresponding nanocomposites based on PP and PA. The deformability of the intercalated nanocomposite decreases by more than 4 times, whereas for the exfoliated nanocomposite, deformability is somewhat preserved, resulting in a twofold reduction in  $\varepsilon$ .

For polymer blends, considering the incorporation of the respective nanocomposites, the followings can be stated. The modulus of elasticity for these blends takes an intermediate position according to the rule of additives. Enhancement of interfacial adhesion through the introduction of a compatibilizer in the form of PP-g-MA (formation of grafted copolymer of PA with PP at the phase interface) leads to a 20% increase in Young's modulus. Replacing PP with intercalated nanocomposite, PA with exfoliated nanocomposite, and their simultaneous replacement without a compatibilizer revealed increases in the modulus of elasticity by 28, 40, and 44 %, respectively. Of particular significance is the composition involving PA/PP/clay, which exhibits a remarkable combination of high elastic modulus and noticeable plasticity.

TABLE 3. Mechanical properties of the blends and components

	$E$ , [MPa]	$\sigma$ , [MPa]	$\varepsilon$ , [%]
PP	$854 \pm 49$	$32.5 \pm 0.9$	$371 \pm 53$
PPClay	$929 \pm 65$	$33.6 \pm 2.6$	$84 \pm 31$
PA	$973 \pm 31$	$58.2 \pm 2.1$	$222 \pm 39$
PAClay	$1477 \pm 68$	$66.9 \pm 2.3$	$112 \pm 33$
PA/PP	$896 \pm 69$	$38.5 \pm 2.3$	$18 \pm 6$
PA/PP/PP-g-MA	$1075 \pm 20$	$43.3 \pm 5.5$	$50 \pm 7$
PA/PPClay	$1148 \pm 96$	$53.1 \pm 2.6$	$356 \pm 39$
PAClay/PP	$1254 \pm 75$	$43.6 \pm 9.7$	$9 \pm 4$
PAClay/PPClay	$1290 \pm 58$	$47.3 \pm 1.4$	$23 \pm 7$

#### 4. Conclusion

In this paper, we studied the rheological, morphological and mechanical properties of PA and PP blends in the presence of layered silicates. The melt viscosity of nanocomposites is highly influenced by the dispersion of layered silicate particles, exfoliated PA nanocomposites exhibited notably higher viscosity compared to intercalated PP nanocomposites. In the blends, the introduction of a compatibilizer or nanocomposites derived from original components always increases complex viscosity. In terms of morphology, the PA/PPClay blend indicates the most finely dispersed morphology rather than PAClay/PP or the blend with traditional PP-g-MA. The increased viscosity of the PPClay leads to an equal amount of viscosity of the blend components, in turn; this will create the necessary condition for dispersion of minor phase particles. Moreover, intercalated clay particles and PP-g-MA, in the PPClay content, avoid agglomeration because they tend to interact with PA molecules. As to PAClay/PP blend, as long as particles with  $10 \mu\text{m}$  there are also nanosized particles and better dispersion of PP dispersed phase too. Even though the occurrence of interaction between PP and clay particles, in the PAClay content, is not possible, better dispersion than pure blend was caused due to the higher viscosity of PAClay. The increase of matrix viscosity resists coalescence and particularly thanks to this reason PAClay/PP indicates more finer dispersed morphology than PA/PP blend. With regard to mechanical properties, compatibilization enhances all mechanical characteristics relative to the blend with pure components while all blends with clay are superior to compatibilized one. Due to the advantage of PA/PPClay in terms of dispersion, it has the highest values of  $\sigma$  and  $\varepsilon$  amongst all blends obtained while blends with PAClay are dominant by elastic modulus.

#### References

- [1] Begum S.A., Rane A.V., & Kanny K. Applications of compatibilized polymer blends in automobile industry. *Compatibilization of polymer blends*, 2020, P. 563–593.
- [2] Annandarajah C., Langhorst A., Kiziltas A., Grewell D., Mielewski D., & Montazami R. Hybrid cellulose-glass fiber composites for automotive applications. *Materials*, 2019, **12**(19), P. 3189.
- [3] Tokumitsu K., Nakajima Y., & Aoki K. Mechanical properties of PP/PA blends in addition with PP-g-MAH with different PP molecular weight and MAH content. *AIP Conference Proceedings*, 2016, **1713**(1).
- [4] Sehanobish K. *Engineering plastics and plastic composites in automotive applications*, 2009, Vol. 122.
- [5] Occhiello E., Giannotta G., Penco M., Garbassi F. Interfacial adhesion in incompatible polymer blends. *First International Congress on Adhesion Science and Technology*, 2000, **1**(3), P. 693–702.
- [6] Mostafapoor F., Khosravi A., Fereidoon A., Khalili R., Jafari S.H., Vahabi H., & Saeb M.R. Interface analysis of compatibilized polymer blends. *Compatibilization of Polymer Blends*, 2020, P. 349–371.
- [7] Jordan A.M., Kim K., Bates F.S., Macosko C.W., Jaffer S., & Lhost O. Rheological characterization and thermal modeling of polyolefins for process design and tailored interfaces. *AIP Conference Proceedings*, 2017, **1843**(1). AIP Publishing.
- [8] Ubonnut L., Thongyai S., & Praserttham P. Interfacial adhesion enhancement of polyethylene–polypropylene mixtures by adding synthesized diisocyanate compatibilizers. *Journal of applied polymer science*, 2007, **104**(6), P. 3766–3773.
- [9] Ajitha A.R., & Thomas S. Compatibilization of polymer blends. *Compatibilization of Polymer Blends*, 2019, **640**.
- [10] Zhang W., Gui Z., Lu C., Cheng S., Cai D., & Gao Y. Improving transparency of incompatible polymer blends by reactive compatibilization. *Materials Letters*, 2013, **92**, P. 68–70.
- [11] Nguyen-Tran H.D., Hoang V.T., Do V.T., Chun D.M., & Yum Y.J. Effect of multiwalled carbon nanotubes on the mechanical properties of carbon fiber-reinforced polyamide-6/polypropylene composites for lightweight automotive parts. *Materials*, 2018, **11**(3), P. 429.
- [12] Xu M., Lu J., Qiao Y., Wei L., Liu T., Lee P.C., ... & Park C.B. Toughening mechanism of long chain branched polyamide 6. *Materials & Design*, 2020, **196**, P. 109173.
- [13] Jang H.G., Yang B., Khil M.S., Kim S.Y., & Kim J. Comprehensive study of effects of filler length on mechanical, electrical, and thermal properties of multi-walled carbon nanotube/polyamide 6 composites. *Composites Part A: Applied Science and Manufacturing*, 2019, **125**, P. 105542.

- [14] Ghanta T.S., Aparna S., Verma N., & Purnima D. Review on nano- and microfiller-based polyamide 6 hybrid composite: Effect on mechanical properties and morphology. *Polymer Engineering & Science*, 2020, **60**(8), P. 1717–1759.
- [15] Raji M., Mekhzoum M.E.M., Rodrigue D., & Bouhfid R. Effect of silane functionalization on properties of polypropylene/clay nanocomposites. *Composites Part B: Engineering*, 2018, **146**, P. 106–115.
- [16] Berdinazarov Q.N., Khakberdiev E.O., Normurodov N.F., & Ashurov N.R. Mechanical and Thermal Degradation Properties of Isotactic Polypropylene Composites with Cloisite15A and Cloisite20A. *Bulletin of the University of Karaganda – Chemistry*, 2022, **3**.
- [17] Banerjee S.S., Janke A., Gohs U., & Heinrich G. Electron-induced reactive processing of polyamide 6/polypropylene blends: Morphology and properties. *European Polymer Journal*, 2018, **98**, P. 295–301.
- [18] Hasanpour M., Razavi Aghjeh M.K., Mehrabi Mazidi M., & Afsari B. Effect of morphology alteration on mechanical properties and fracture toughness of polypropylene/polyamide 6/ethylene polypropylene diene monomer graft maleic anhydride (PP/PA6/EPDM-g-MA) reactive ternary blends. *Polymer Bulletin*, 2020, **77**, P. 3767–3794.
- [19] Afshari M., Kotek R., Haghighat Kish M., Nazock Dast H., & Gupta B.S. Effect of blend ratio on bulk properties and matrix–fibril morphology of polypropylene/nylon 6 polyblend fibers. *Polymer*, 2002, **43**(4), P. 1331–1341.
- [20] Rocha J.A., Steffen T.T., Fontana L.C., & Becker D. Effect of maleic anhydride and oxygen functionalized carbon nanotube on polyamide 6 and polypropylene blend properties. *Polymer Bulletin*, 2021, **78**, P. 5623–5639.
- [21] Motamedi P., & Bagheri R. Modification of nanostructure and improvement of mechanical properties of polypropylene/polyamide 6/layered silicate ternary nanocomposites through variation of processing route. *Composites Part B: Engineering*, 2016, **85**, P. 207–215.
- [22] Motamedi P., & Bagheri R. Investigation of the nanostructure and mechanical properties of polypropylene/polyamide 6/layered silicate ternary nanocomposites. *Materials & design*, 2010, **31**(4), P. 1776–1784.
- [23] Ou B., Li D., & Liu Y. Compatibilizing effect of maleated polypropylene on the mechanical properties of injection molded polypropylene/polyamide 6/functionalized-TiO<sub>2</sub> nanocomposites. *Composites science and technology*, 2009, **69**(3-4), P. 421–426.
- [24] Chow W.S., Mohd Ishak Z.A., & Karger, J. Morphological and rheological properties of polyamide 6/poly (propylene)/organoclay nanocomposites. *Macromolecular Materials and Engineering*, 2005, **290**(2), P. 122–127.
- [25] Khakberdiev E.O., Berdinazarov Q.N.U., Toshmamatov D.A.U., & Ashurov N.R. Mechanical and morphological properties of poly (vinyl chloride) and linear low-density polyethylene polymer blends. *Journal of Vinyl and Additive Technology*, 2022, **28**(3), P. 659–666.
- [26] De Almeida F., Correia A., e Silva E.C., Lopes I.C., & Silva F.J.G. Compatibilization effect of organophilic clays in PA6/PP polymer blend. *Procedia Manufacturing*, 2018, **17**, P. 1154–1161.
- [27] Harrats C., Omonov T., Groeninckx G., & Moldenaers P. Phase morphology development and stabilization in polycyclohexylmethacrylate/polypropylene blends: uncompatibilized and reactively compatibilized blends using two reactive precursors. *Polymer*, 2004, **45**(24), P. 8115–8126.
- [28] Hsissou R., Bekhta A., Dagdag O., El Bachiri A., Rafik M., & Elharfi A. Rheological properties of composite polymers and hybrid nanocomposites. *Heliyon*, 2020, **6**(6).
- [29] Zeng N., Bai S.L., G'sell C., Hiver J.M., & Mai Y.W. Study on the microstructures and mechanical behaviour of compatibilized polypropylene/polyamide-6 blends. *Polymer International*, 2002, **51**(12), P. 1439–1447.
- [30] Saikrishnan S., Jubinville D., Tzoganakis C., & Mekonnen T.H. Thermo-mechanical degradation of polypropylene (PP) and low-density polyethylene (LDPE) blends exposed to simulated recycling. *Polymer Degradation and Stability*, 2020, **182**, P. 109390.
- [31] Aparna S., Purnima D., & Adusumalli R.B. Review on various compatibilizers and its effect on mechanical properties of compatibilized nylon blends. *Polymer-Plastics Technology and Engineering*, 2017, **56**(6), P. 617–634.
- [32] Liu L., Qi Z., & Zhu X. Studies on nylon 6/clay nanocomposites by melt-intercalation process. *Journal of Applied Polymer Science*, 1999, **71**(7), P. 1133–1138.

---

Submitted 27 October 2023; revised 31 January 2024; second revision 3 April 2024; third revision 11 June 2024;  
accepted 12 June 2024

#### Information about the authors:

*Qodirbek Nuridin ugli Berdinazarov* – Institute of Polymer Chemistry and Physics, Uzbekistan Academy of Sciences, A. Kadyri str. 7b, 100128, Tashkent, Uzbekistan; ORCID 0000-0002-4422-2305; qodirberdinazarov@mail.ru

*Elshod Olmosovich Khakberdiev* – Institute of Polymer Chemistry and Physics, Uzbekistan Academy of Sciences, A. Kadyri str. 7b, 100128, Tashkent, Uzbekistan; ORCID 0000-0002-7707-2219; profhaqberdiyev@gmail.com

*Nigmat Rustamovich Ashurov* – Institute of Polymer Chemistry and Physics, Uzbekistan Academy of Sciences, A. Kadyri str. 7b, 100128, Tashkent, Uzbekistan; ORCID 0000-0003-0765-5942; nigmat.ashurov@gmail.com

*Conflict of interest:* the authors declare no conflict of interest.